

Recoupling Diagrams for Duality

G. P. Canning

Instituut voor Theoretische Fysica, Universiteit Leuven, Celestijnenlaan, 200D, B-3030 Heverlee, Belgium

(Received 15 November 1972)

We show how duality diagrams may be rigorously formulated in terms of recoupling diagrams. This allows us to write down in closed form general solutions to the constraints imposed by duality and the absence of exotic resonances, and to give for the first time in closed form general expressions for the coupling constants in terms of the quark-hadron recoupling coefficients which are given by the $6j$ -like symbols of the appropriate group. We note the connection with the internal-symmetry factors given by the trace of a product of matrices, and we further note that $SU(n)$ is not determined by the above constraints.

I. INTRODUCTION

For $SU(2)$, diagrammatic techniques have been developed for the handling of Clebsch-Gordan coefficients $3j$, $6j$, and multi- j symbols by Yutsis *et al.*,¹ Kotański *et al.*,² and Massot *et al.*³ These techniques have been further developed for $SU(3)$ by El-Baz *et al.*^{4,5}

From the concepts built into these symbols for recoupling coefficients, it is clear that such diagrams may be applied to any group whose products of representations have well-defined Clebsch-Gordan series, and the symmetries of these coefficients will be similar provided that the representations can be expressed in terms of Young diagrams.

These diagrammatic techniques allow us to formulate the duality diagrams of Rosner⁶ and Harari⁷ in a rigorous way as a solution to the crossing constraints imposed by duality and the absence of exotic resonances. We can then give closed form diagrammatic expressions for the coupling constants in terms of the recoupling coefficients ($6j$ -like symbols) of the appropriate group.

Apart from the particularities of the phase factors involved [for $SU(2)$ see Edmonds,⁸ and for $SU(3)$ see de Swart⁹] which are convention-dependent, the results are quite independent of the group structure assumed. For this reason, in what follows, we shall not do the bookkeeping associated with these phases. These can be worked out by hand and they should not affect relative phases.

Before writing down the duality diagrams as recoupling diagrams, we first give just a brief introduction to the use of these diagrams in Sec. II. We refer the reader to Refs. 1-5 for details of the diagrammatic techniques, and to Refs. 8 and 9 for detailed nondiagrammatic treatment. From these authors, the reader may learn how to include the correct phases in the particular cases

of $SU(2)$ and $SU(3)$.

In Sec. III we give a general treatment for meson duality diagrams, and in Sec. IV for baryon-meson duality diagrams containing just one $B\bar{B}$ pair and many mesons. In Sec. V we present our conclusions.

In the Appendix we comment on the construction of fully symmetrized $3jm$ -type symbols and $6j$ -type symbols for a general group from the Clebsch-Gordan coefficients of that group.

II. METHOD

We start from the Clebsch-Gordan coefficient for the given group:

$$\begin{pmatrix} \mu_1 & \mu_2 & \mu_3 \gamma \\ \nu_1 & \nu_2 & \nu_3 \end{pmatrix}, \quad (1)$$

where μ_i labels the representation; ν_i labels the particular state within the representation by means of other quantum numbers, some additive and some not; and γ labels a particular orthogonal state in the case where μ_3 occurs more than once in the product $\mu_1 \times \mu_2$. The set

$$\begin{pmatrix} \mu_3 \gamma \\ \nu_3 \end{pmatrix}$$

form a complete orthonormal basis for all the states in the product $\mu_1 \times \mu_2$. Such states will normally be chosen so as to have a defined symmetry under the interchange $\mu_1 \leftrightarrow \mu_2$.

In what follows, Eqs. (4) and (5) appear both in conventional form in the text and in diagrammatic form in Fig. 1. Subsequent equations of this section and of other sections are grouped into a figure since they cannot be handled typographically. In these diagrams juxtaposed symbols are to be multiplied together unless otherwise indicated.

The partially symmetrized Clebsch-Gordan coefficient is represented diagrammatically by Eq. (2) shown in Fig. 1. Here $[\mu]^2$ denotes the dimension of the representation μ , and \pm indicates

the anticyclic/cyclic ordering of the representations in the Clebsch-Gordan coefficient. A reversed arrow would indicate the conjugate representation entering with a phase factor appropriate to the contragredient representation.

A line between two vertices implies a summation equivalent to a contraction of spherical tensor indices, as shown in Eq. (3). The fact that the $|\mu_\nu^\gamma\rangle$ form a complete orthonormal set allows us to write two orthogonality relations as follows:

$$\sum_{\mu, \nu, \gamma} \begin{pmatrix} \mu_1 & \mu_2 & \mu & \gamma \\ \nu_1 & \nu_2 & \nu & \end{pmatrix} \begin{pmatrix} \mu & \gamma & \mu_1 & \mu_2 \\ \nu & & \nu_1 & \nu_2 \end{pmatrix} = \delta_{\nu_1 \nu_1'} \delta_{\nu_2 \nu_2'} \quad (4)$$

$$\sum_{\nu_1, \nu_2} \begin{pmatrix} \mu_1 & \mu_2 & \mu & \gamma \\ \nu_1 & \nu_2 & \nu & \end{pmatrix} \begin{pmatrix} \mu & \gamma & \mu_1 & \mu_2 \\ \nu & & \nu_1 & \nu_2 \end{pmatrix} = \delta_{\mu \mu'} \delta_{\nu \nu'} \delta_{\gamma \gamma'} \quad (5)$$

These two identities may be thought of as coming from the cutting of the line(s) in the identity shown in Eq. (6). Combining expressions (4) and (5) in more complicated diagrams, we may obtain the general type of identity shown in Eq. (7) as given by Kotański² and El-Baz,⁵ and also, in particular, the very useful identity of Eq. (8). In the case of SU(2), the closed line symbol in Eq. (8) is just a δ_j symbol (up to a phase factor).

In general, in the terminology of Ref. 3, a dia-

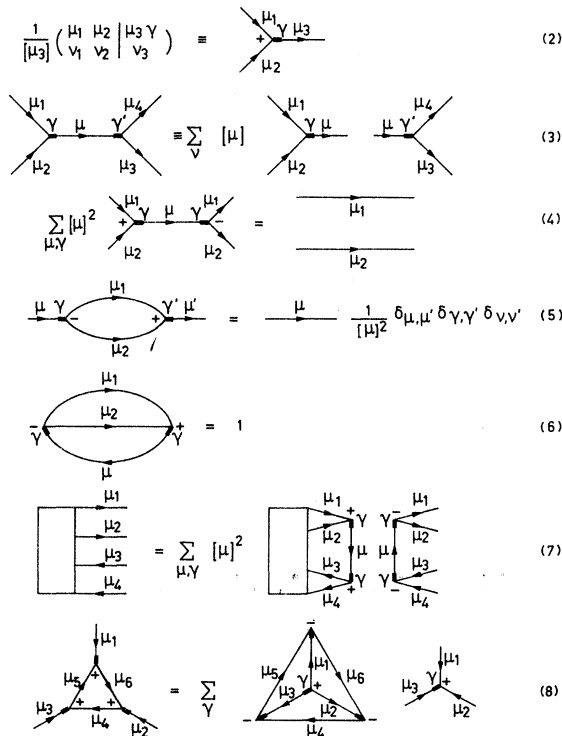


FIG. 1. Diagrammatic equations (2)–(8) of Sec. II.

gram with n legs and no loops is an njm symbol and a diagram with n lines and no external lines is an nj symbol. A diagram with n legs and loop(s) may be reduced to a product of an njm symbol and an $n'j$ symbol (with summations over intermediate j 's where required) by identities of the general type of Eq. (7).

III. MESON DUALITY DIAGRAMS

We begin with the well-known 4-point meson diagram, and we first derive the crossing matrix diagrammatically, as shown in Eq. (9) (see Fig. 2)

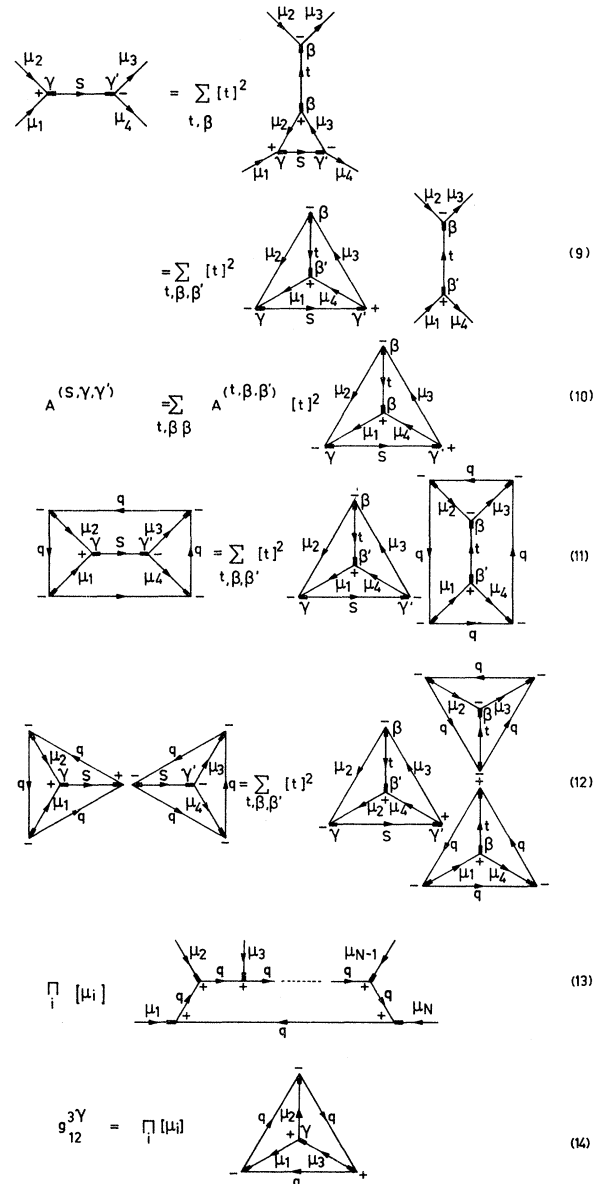


FIG. 2. Diagrammatic equations (9)–(14) of Sec. III.

by use of Eqs. (4) and (8). Thus our problem is to solve Eq. (10), in which $A^{(s;\gamma,\gamma')}$ and $A^{(t;\beta,\beta')}$ are the s - and t -channel reduced amplitudes, in such a way that s and t extend only over the nonexotic representations and in such a way that the resonance dominated amplitudes always give factorizable couplings.

Now from Eq. (9) we clearly have the diagrammatic identity given in Eq. (11), in which q denotes the quark representation used to define nonexotic mesons as $q\bar{q}$ and baryons as qqq . Moreover, the multi- j type symbols of Eq. (11) factorize by use of Eq. (8) to give Eq. (12); for SU(2) this is just the Biedenharn-Elliot sum rule for $6j$ symbols, as given in Ref. 8. We can now see by inspection of Eq. (12) that we have indeed found a solution to Eq. (10) having the desired properties of absence of exotic channels and factorization of the nonexotic resonating channels.

The above forms the basis for the diagrammatic solution to the crossing constraints imposed by duality. Thus for the N -meson duality diagram, we write (in a more symmetrical way) the expression in Eq. (13). We make use of the identities of the general type of Eq. (7) to factorize

$$\square \times \square \times \square = \square + \square + \square + \square \quad (15)$$

$$\sum_Q C(B,Q) \begin{array}{c} q \\ \diagup \quad \diagdown \\ B \quad \quad \quad q \\ \diagdown \quad \diagup \\ q \end{array} \quad (16)$$

$$\begin{array}{c} q \\ \diagup \quad \diagdown \\ q \quad \quad \quad q \\ \diagdown \quad \diagup \\ q \end{array} = \delta_{q,q'} \frac{1}{[q]^2} \quad (17)$$

$$\begin{array}{c} q \\ \diagup \quad \diagdown \\ q \quad \quad \quad q \\ \diagdown \quad \diagup \\ q \end{array} = \sum_{B,Q} [C(B,Q)[q][B]^2] \times \begin{array}{c} q \\ \diagup \quad \diagdown \\ B \quad \quad \quad q \\ \diagdown \quad \diagup \\ q \end{array} \quad (18)$$

$$\sum_Q C(B,Q) \begin{array}{c} q \\ \diagup \quad \diagdown \\ q \quad \quad \quad \bar{B} \\ \diagdown \quad \diagup \\ q \end{array} \quad (19)$$

$$[B_1][M_2] \dots [B_{k-1}][B_k][M_{k+1}] \dots [M_n] \sum_{Q_1, Q_k} C(B_1, Q_1) C(B_k, Q_k) [Q_1][Q_k] \times \begin{array}{c} M_1 \quad \quad \quad M_{k-1} \\ \diagdown \quad \diagup \quad \quad \quad \diagdown \quad \diagup \\ q \quad \quad \quad q \quad \quad \quad q \quad \quad \quad q \\ \diagup \quad \diagdown \quad \quad \quad \diagup \quad \diagdown \\ B_1 \quad \quad \quad q \quad \quad \quad q \quad \quad \quad \bar{B}_k \\ \diagdown \quad \diagup \quad \quad \quad \diagdown \quad \diagup \\ M_n \quad \quad \quad M_{k+1} \end{array} \quad (20)$$

FIG. 3. Diagrammatic equations (15)–(20) of Sec. IV.

Eq. (13) into a particular tree-graph njm coefficient and a multi- j graph. Then using Eq. (8) we shall factorize the multi- j graph into a product of $6j$ -like symbols, one for each 3-point vertex of the tree graph. This gives the closed form of Eq. (14) for the 3-meson reduced coupling.

The coupling for a definite signature point on the α_3 trajectory is then given by $g_{12}^{3\gamma} + \sigma_3 g_{21}^{3\gamma}$, and if γ is chosen so as to be even or odd under interchange $\mu_1 \leftrightarrow \mu_2$, then we shall find the linking of the internal symmetry and the configuration space symmetry as required by Bose statistics for self-conjugate mesons.

We note that the solution given by Eq. (13) is not a model solution, but is the unique solution to the multiparticle crossing constraints; just as we derived diagrammatically the crossing equation for the 4-point amplitude, so we can derive the multi-particle crossing equations using the diagrammatic methods of Kotanski,¹⁰ and we can then formulate the diagrammatic solution given in Eq. (13). For, by choosing various representations to replace the q 's in Eq. (11), we can obtain a whole set of solutions to Eq. (10) (probably a complete set), but only the one solution which we have singled out has the properties we require of it—and it is for this reason that we can claim that the quarks are introduced into the duality diagrams in a model-independent way.

IV. BARYON DUALITY DIAGRAMS

For baryons the solutions to the crossing equations may be obtained by essentially the same techniques as in Sec. III, except that in the Clebsch-Gordan series $q \times q \times q$ of Eq. (15) (see Fig. 3), we note that the second representation on the right-hand side will always occur twice; and so we have for the coupling to a given baryon B a nonunique expression (16). Here the $C(B, Q)$ are suitable coupling coefficients which cannot, unfortunately, be represented diagrammatically, and here, as in subsequent equations, the summation over Q will refer to the representations in the Clebsch-Gordan series for $q \times q$, and a summation over B will refer to the representation occurring twice in $q \times q \times q$.

By analogy with Eq. (6), the identity Eq. (17) allows us to write, analogously to Eq. (4), Eq. (18), which may also be derived directly from the application of Eq. (4) twice. Note: In the space of the orthogonal baryon states in the representation which occurs twice in $q \times q \times q$ and in the space of the representations Q lying in $q \times q$, we require also for factorization the following subsidiary orthogonality conditions on the coefficients C :

$$\sum_B C(B, Q) C(B, Q') = \delta_{Q, Q'}$$

$$\sum_Q C(B, Q) C(B', Q) = \delta_{B, B'}$$

Equation (18) also serves to identify the conjugate antibaryon \bar{B} , shown in Eq. (19).

The general solution to the planar crossing constraints is then given by the expression (20). We may then check, using the diagrammatic techniques at our disposal, in particular Eqs. (4) and (18), that Eq. (20) then gives for the $B_1 M_2 \bar{B}_3$ vertex Eq. (21) in Fig. 4, in which we have used Eq. (5) to simplify the expression we first obtain. For the $M_2 B_1 \bar{B}_3$ vertex we find Eq. (22), in which we use Eq. (8) to simplify the expression we first obtain.

We thus obtain coupling constants satisfying our conditions, but we note that baryon trajectories will not necessarily have defined signature, for $g_{12}^{3Y} + \sigma_3 g_{21}^{3Y}$ will no longer exhibit the same simple symmetry linked with representation as for mesons. This illustrates the fundamental phenomenological problem of planar duality for meson-baryon amplitudes, namely that where B lies in the representation appearing twice in $q \times q \times q$ (i.e., where the summation over Q is not trivial), the signature linked with representation no longer holds—and this leads to predictions for unsigned baryon trajectories which have never yet been observed; see Refs. 11–14.

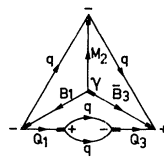
We might also draw recoupling diagrams for the nonplanar duality constraints of Mandelstam¹³ of the type shown in Eq. (23), and in this case we find the same two types of coupling for $BM\bar{B}$ and $MB\bar{B}$ as may be checked by analyzing the diagram graphically. We can see, however, no valid reason for introducing crossed diagrams such as Eq. (24) because these diagrams introduce couplings like those in Eq. (25) and they cannot be projected out in a self-consistent way by use of Eq. (18) for all vertices; their inclusion would not allow consistent factorizable 3-point couplings to be obtained. For the same reason we do not include the η -like coupling of Eq. (26) which arises from two such twists.

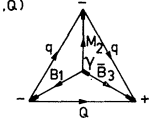
V. CONCLUSIONS

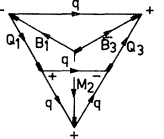
Our main conclusion is that quark duality diagrams may be given a rigorous mathematical formulation in terms of recoupling diagrams for general quarks. This allows us to write down in closed form the solution to the crossing constraints imposed by duality and the absence of exotic resonances given in Eqs. (13) and (20). Likewise this also gives us in closed form the coupling constants of Eq. (15) and Eqs. (21) and

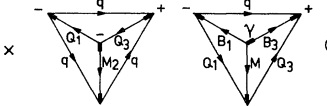
(22) which may be evaluated in terms of the $6j$ -like symbols of the appropriate group.

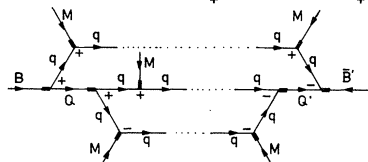
We note that the sum over spherical-tensor indices in the duality diagrams of Eqs. (13) and (20), as defined in Eq. (3), can be rewritten in terms of the trace of a product of matrices, whose indices are just the spherical tensor indices ap-

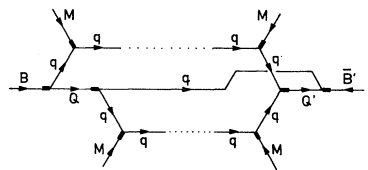
$$g_{12}^{3Y} = [B_1][M_2][\bar{B}_3] \sum_{Q_1, Q_3} C(B_1, Q_1) C(B_3, Q_3) [Q_1][Q_3]$$


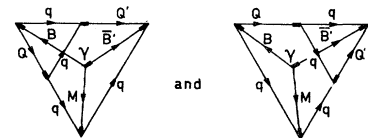
$$= [B_1][M_2][\bar{B}_3] \sum_Q C(B_1, Q) C(B_3, Q)$$

(21)

$$g_{21}^{3Y} = [B_1][M_2][B_3] \sum_{Q_1, Q_3} C(B_1, Q_1) C(B_3, Q_3) [Q_1][Q_3]$$


$$= [B_1][M_2][B_3] \sum_{Q_1, Q_3} C(B_1, Q_1) C(B_3, Q_3) [Q_1][Q_3]$$

(22)


(23)


(24)


(25)


(26)

FIG. 4. Diagrammatic equations (21)–(26) of Sec. IV.

pearing in the Clebsch-Gordan coefficients. For the case of mesons only as in Eq. (13), we find the Paton-Chan isospin factor,¹⁵ and in the case of mesons and baryons as in Eq. (20), we find the extension in terms of rectangular matrices and block-diagonal matrices of Ref. 14. The diagrammatic formulation makes the group symmetry of the couplings manifest, and the matrix formulation makes the factorizability of the couplings manifest.

We further conclude that the only *a priori* constraints on the group symmetry of the coupling constants bootstrapped by dual dynamics is that the group should have a well-defined Clebsch-Gordan series for the products of its representations. This supports the thesis of Van Parijs *et al.*,¹⁶ who show by the specific example of SO(5) that the group need not be SU(*n*). This conflicts with the thesis of Capps¹⁷ and Dethlefsen *et al.*¹⁸ However, where we expect the internal symmetry [except for the subgroup of SU(2) of isospin] to be broken by giving some of the quarks a heavier mass, we believe that the final result will "look more like a broken SU(*n*)."¹⁹

Lastly a footnote: It is now manifestly clear why in a quark dual diagram for a 3-point meson coupling, each quark must be exchanged and not turn back on itself. Since the lines properly imply a sum on the quark indices, such a diagram would be valid only where the meson lay in the representation $1 \sim \sum_i q_i \bar{q}_i$; otherwise the coupling would not even conserve the symmetry.

APPENDIX: THE 3j COEFFICIENT

We use the results Eq. (27) (see Fig. 5) to derive from the crossing equation Eq. (9) the further results that follow when one of the lines is just the identity representation, and from Eq. (28) so obtained, we derive Eq. (29). Now, using Eq. (29) in the case where the summation over β reduces to one term, we may invert the equation and so derive Eq. (30), from which we then obtain Eq. (31). Hence, where no summation over β is involved, the coefficient in Eq. (29) is merely a phase factor.

Thus in SU(2) where indeed no summation is found, we may, with appropriate phase conventions, define 3j m symbols having the full symmetry required under the interchange of all the columns in the coefficient. In SU(3) the summation is quite often not found (in particular, where one of the representations is the fundamental one), and in the particularly important case of 8 \times 8, by choosing the totally symmetric and totally anti-symmetric

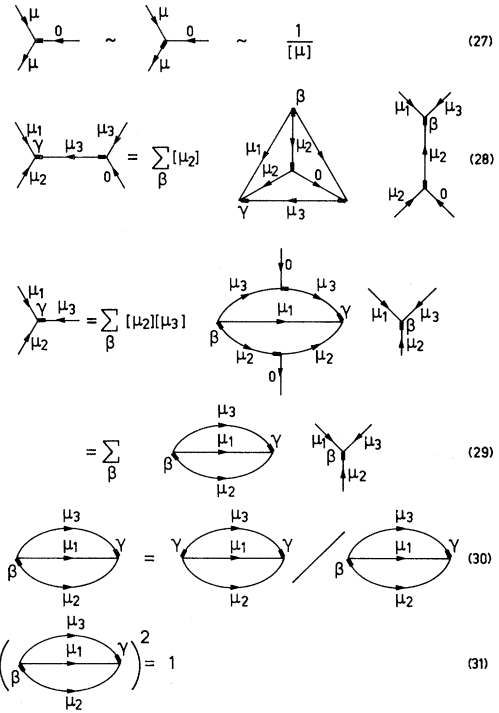


FIG. 5. Diagrammatic equations (27)–(31) of the Appendix.

$$\left(\begin{array}{c|c} 8_1 & 8_3 \\ \nu_1 & \nu_3 \end{array} \middle| \begin{array}{c} 8_3 \\ \nu_3 \end{array} \right)$$

(corresponding to the familiar d_{ijk} and f_{ijk}), we again find the summation restricted so that either the symmetric γ or the antisymmetric γ can occur in the coefficient in Eq. (29). Hence we may, as stated by de Swart,⁹ obtain the full symmetry under the interchange of all the columns in the Clebsch-Gordan coefficient—at least in some cases, which would be required in order to be able to construct 3 μ symbols. But it is still not clear whether this can be done in general by suitable choices of γ 's.

Our notation is thus designed so that (where possible) the permutation of any pair of legs or indeed the changing of the position of the thick bar (denoting the representation onto which the two others are projected) in Eq. (2) will lead to a phase dependent on the μ_i but not on the ν_i . Hence the 6j-type symbols appearing in the coupling constants will differ by only a phase from those defined by some other convention, and the usual permutations of the representations may be made—although the phases may be nonstandard. In particular, provided the implicit summations prescribed by the 6j-type diagrams are correctly

carried out, then the ratios of the coupling constants will have the correct phases.

The choice of phase corresponds to that chosen

by Dürr and Wagner²⁰ for SU(2) (in that reference, the reader will also find an account of the use of diagrammatic techniques for γ algebras).

¹A. P. Yutsis, I. B. Levinson, and V. Vanagas, *Mathematical Apparatus of the Theory of Angular Momentum* (Israel Program for Scientific Translation, Jerusalem, Israel, 1962).

²A. Kotański and K. Zalewski, *Acta Phys. Pol.* **XXVI**, 109 (1964).

³J. N. Massot, E. El-Baz, and J. Lafoucrière, *Rev. Mod. Phys.* **39**, 288 (1967).

⁴E. El-Baz, B. Castel, J. N. Massot, and J. Lafoucrière, *Nucl. Phys.* **B2**, 51 (1967).

⁵E. El-Baz and B. Castel: *Graphical Methods of Spin Algebras in Atomic, Nuclear, and Particle Physics* (Marcel Dekker, New York, 1972).

⁶J. L. Rosner, *Phys. Rev. Lett.* **22**, 689 (1969).

⁷H. Harari, *Phys. Rev. Lett.* **22**, 562 (1969).

⁸A. R. Edmonds, *Angular Momentum in Quantum Mechanics* (Princeton University Press, Princeton, New Jersey, 1957).

⁹J. J. de Swart, *Rev. Mod. Phys.* **35**, 916 (1963).

¹⁰A. Kotanski and K. Zalewski, *Acta Phys. Pol.* **XXVI**, 117 (1964).

¹¹J. Mandula, C. Rebbi, R. Slanski, J. Weyers, and G. Zweig, *Phys. Rev. Lett.* **22**, 1147 (1969).

¹²R. H. Capps, *Phys. Rev. Lett.* **22**, 215 (1969).

¹³S. Mandelstam, *Phys. Rev. D* **1**, 1734 (1969).

¹⁴G. P. Canning, Leuven report, 1972 (unpublished).

¹⁵J. E. Paton and Chan Hong-Mo, *Nucl. Phys.* **B10**, 516 (1969).

¹⁶J. Van Parijs, D. Speiser, and J. Weyers, *Nuovo Cimento* **11A**, 295 (1972).

¹⁷R. H. Capps, *Phys. Rev. D* **3**, 3059 (1971).

¹⁸J. Dethlefsen and H. B. Nielsen, *Nuovo Cimento* **14A**, 85 (1973).

¹⁹G. P. Canning, Leuven report, 1972 (unpublished).

²⁰H. P. Dürr and F. Wagner, *Nuovo Cimento* **53A**, 255 (1968).

Cabibbo Angle and Rotation Projection*

William F. Palmer

Department of Physics, The Ohio State University, Columbus, Ohio 43210

(Received 2 April 1973)

The hadron Hamiltonian for strong and nonleptonic weak interactions is regarded as a function of the Cabibbo angle, evolving from a primitive "initial condition" (in which weak and strong hypercharge are identical) to its physical value by a rotation projection. Various existing determinations of the Cabibbo angle are reproduced and a new one is calculated, with good numerical results for an initial condition in which chiral SU(2) is broken only by an octet term in the electromagnetic direction.

The nonleptonic weak, electromagnetic, and semistrong interactions of hadrons define, through their SU(3) breaking,¹ an SU(3) frame orientation for the description of purely hadronic processes. Regarding for the moment the weak hypercharge and electric charge as fixed, "external" field directions which provide a coordinate system with which to probe the strong-interaction Hamiltonian, $H_S(\theta)$, where θ is the Cabibbo angle, let us consider a theory in which $H_S(\theta)$ continuously evolves from $H_S(0)$.

$$H_S(\theta) = \mathcal{K}[H_S(0)]. \quad (1)$$

If $H_S(\theta) = H_S^{(0)}(\theta) + H_S^{(8)}(\theta)$ is octet-broken for all θ , and is on the same SU(3) orbit² for all θ , there is

an SU(3) transformation

$$U(\theta) \equiv e^{-2i\epsilon_i(\theta)F_i}, \quad U(0) = 1$$

such that

$$H_S(\theta) = U(\theta)H_S(0)U^\dagger(\theta). \quad (2)$$

Otherwise (and this is the case of physical interest),

$$\begin{aligned} H_S(\theta) &= U(\theta)[H_S(0) + \tilde{G}(\theta)]U^\dagger(\theta) \\ &= U(\theta)H_S(0)U^\dagger(\theta) + G(\theta) \\ &= \mathcal{K}[H_S(0)], \end{aligned} \quad (3)$$

where $G(\theta)$ is the orbit shift. This allows $H_S(\theta)$ to interpolate between, say, an SU(2) \times U(1) orbit for